

# Blue Supergiants as a Tool for Extragalactic Distances – Empirical Diagnostics\*

Fabio Bresolin

Institute for Astronomy, University of Hawaii, Honolulu HI 96822, USA

*bresolin@ifa.hawaii.edu*

**Abstract.** Blue supergiant stars can be exceptionally bright objects in the optical, making them prime targets for the determination of extragalactic distances. I describe how their photometric and spectroscopic properties can be calibrated to provide a measurement of their luminosity. I first review two well-known techniques, the luminosity of the brightest blue supergiants and, with the aid of recent spectroscopic data, the equivalent width of the Balmer lines. Next I discuss some recent developments concerning the luminosity dependence of the wind momentum and of the flux-weighted gravity, which can provide, if properly calibrated, powerful diagnostics for the determination of the distance to the parent galaxies.

## 1 Introduction

Massive stars can reach, during certain phases of their post-main sequence evolution, exceptional visual luminosities, approaching  $M_V \sim -10$  in extreme cases. It is thus natural to try and use them as standard candles for extragalactic studies, as was realized long ago by Hubble. For this contribution I will concentrate on the blue supergiants, a rather broad but useful definition for the stars contained in the upper part of the H–R diagram and with spectral types O, B and A. This includes ‘normal’ supergiants (Ia) and hypergiants (Ia<sup>+</sup>), as well as more exotic objects such as the Luminous Blue Variables (LBV’s). Very bright stars can also be found among the yellow hypergiants, however their identification in extragalactic systems is more problematic, because their intermediate color coincides with that of numerous Galactic foreground dwarfs.

From the point of view of the extragalactic distance scale, it is not the most massive, intrinsically most *luminous* O-type stars ( $M_{bol} \leq -11$ ) which are appealing. Because of the decrease of the bolometric correction with temperature from O to A stars down to  $\sim 7000$  K, the *visually brightest* supergiants found in galaxies are mostly 25–40  $M_\odot$  mid-B to early-A type stars, with  $M_{bol}$  between  $-8$  and  $-9$  [48]. This can be seen from Table 1, which is a (probably incomplete) compilation of the visually brightest blue stars in the Milky Way, LMC and SMC, excluding in general LBV’s with maximum light amplitudes larger than 0.5 mag. The label LBV in the last column identifies known or suspected LBV’s, from the compilation of [87]. Sources for the photometry and spectral types are given as a footnote to the table, however in a few cases the data have been updated with more recent determinations. The absolute visual magnitudes have

\* Invited review at the International Workshop on *Stellar Candles for the Extragalactic Distance Scale*, held in Concepción, Chile, December 9–11, 2002. To be published in: *Stellar Candles*, Lecture Notes in Physics (<http://link.springer.de/series/lnpp>), Copyright: Springer-Verlag, Berlin-Heidelberg-New York, 2003

generally been corrected for extinction by assuming the spectral type vs.  $B - V$  color index relation in the MK system given by [45] and  $A_V = 3.1 \times E_{B-V}$ . Stars brighter than  $M_V = -8.0$  in all three galaxies are plotted in the color-magnitude (c-m) diagram of Fig. 1, together with the loci of Ia<sup>+</sup>, Ia and Iab stars, and stellar tracks for 60, 40, 25 and 20  $M_\odot$  from [52].

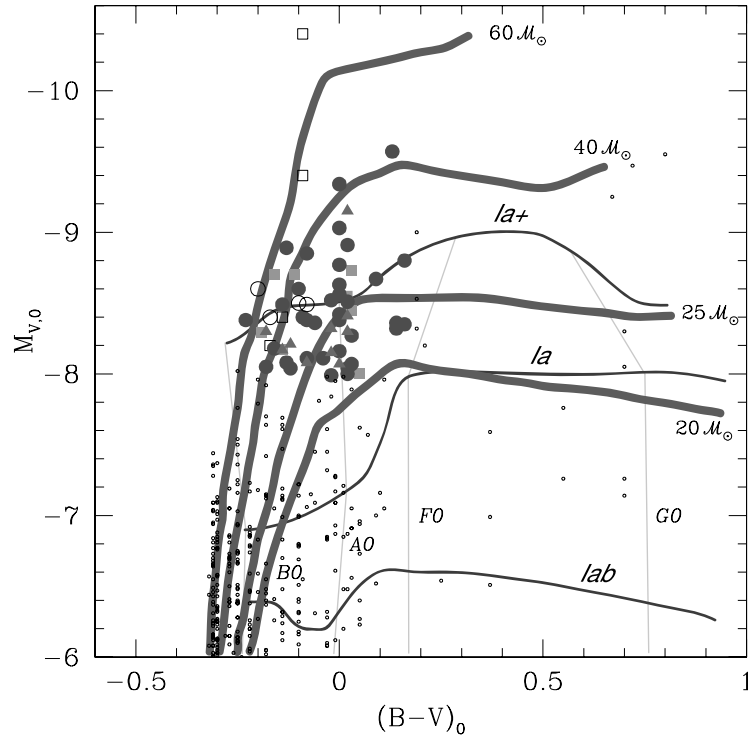


**Fig. 1.** In this color-magnitude diagram the brightest stars having  $M_V < -8$  in the Milky Way (squares), LMC (circles) and SMC (triangles) are shown with the larger symbols. Open symbols refer to confirmed or candidate LBV's with magnitude variations smaller than 0.5 mag. The small points represent Galactic stars fainter than  $M_V = -8$  and/or of spectral type F and later. Schematic evolutionary models at solar metallicity and various ZAMS masses from [52] are shown by the thick lines. The grid giving luminosity classes and spectral types is from [45]

Extragalactic stellar astronomy has quickly evolved from the identification, via photometry and qualitative spectroscopy, of individual bright stars mostly within galaxies of the Local Group, to the quantitative analysis of stellar spectra well beyond the boundaries of the Local Group. The observation and analysis of extragalactic supergiants has important ramifications for the study of massive stellar evolution with mass loss, supernova progenitors, stellar instabilities near the upper boundary of the stellar luminosity distribution, and chemical abundances. Here I review four different techniques concern-

**Table 1.** The visually brightest blue stars in the Milky Way, LMC and SMC

Star ID		$M_{V,0}$	Spectral Type
<b>Milky Way</b>		$M_{V,0} \leq -8.0$	
HD	other		
	Cyg OB2-12	-10.4	B5 Ie LBV
80077		-9.4	B2/3 Ia <sup>+</sup> LBV
92693		-8.73	A2 Ia
152236	$\zeta^1$ Sco	-8.70	B1.5 Ia <sup>+</sup>
	WRA977	-8.7	B1.5 Ia <sup>+</sup>
92207		-8.55	A0 Ia
197345	$\alpha$ Cyg	-8.45	A2 Iae
168607		-8.4	B9 Ia <sup>+</sup> LBV
316285	He3-1482	-8.4	B1e LBV
169454		-8.29	B1 Ia <sup>+</sup>
	MWC314	-8.2	<B2 LBV
92964		-8.17	B2.5 Iae
223385	6 Cas	-8.00	A3 Iae
<b>LMC</b>		$M_{V,0} \leq -8.5$	$m - M = 18.5$
HD	Sk		
33579	-67 44	-9.57	A4 Ia <sup>+</sup>
269902	-69 239	-9.34	B9 Iae
32034	-67 17	-9.03	B9 Iae
270086	-69 299	-8.91	A1 Ia <sup>+</sup>
269546	-68 82	-8.89	B3 Iab
269923	-69 247	-8.85	B6 Iab
269857	-68 131	-8.80	A9 Ia
269781	-67 201	-8.77	A0 Iae
269331	-69 93	-8.67	A5 Ia
268654	-69 7	-8.63	B9 Iae
268835	-69 46	-8.60	B8p
269128	-68 63	-8.6	B2.5 Ia <sup>+</sup> LBV
269661	-69 170	-8.56	B9 Ia <sup>+</sup>
268718	-69 16	-8.52	B9 Iabe
268946	-66 58	-8.51	A0 Ia
37836	-69 201	-8.5	B pec LBV
<b>SMC</b>		$M_{V,0} \leq -8.0$	$m - M = 19.0$
AV	Sk		
475	152	-9.15	A0 Ia <sup>+</sup>
136	54	-8.41	A0 Ia
	56	-8.32	B8 Ia <sup>+</sup>
315	106	-8.30	A0 Ia
78	40	-8.30	B1.5 Ia <sup>+</sup>
443	137	-8.21	B2.5 Ia
56	31	-8.17	B2.5 Ia
65	33	-8.15	B8 Ia <sup>+</sup>
48	27	-8.08	B5 Ia
76	39	-8.07	B9 Ia <sup>+</sup>

SOURCES — MILKY WAY - [34]. Distance to HD 92207, HD 92693, HD 92964 and HD223385: [23]. Cyg OB2-12: [49]. LBV data from [87]. LMC - [67]. SMC - [6], [47].

ing the use of blue supergiants in the context of measuring extragalactic distances. Two of them have quite a long history:

- *luminosity of the brightest blue supergiants*
- *equivalent width of the Balmer lines*

while the two remaining ones are based on more recent developments in the analysis of stellar winds and the atmospheres of blue supergiant stars:

- *the wind momentum–luminosity relationship*
- *the flux-weighted gravity–luminosity relationship*

## 2 The Luminosity of the Brightest Blue Supergiants as a Standard Candle

Since the pioneering work of Hubble [29] a great amount of efforts have been devoted to the calibration of the luminosity of the visually brightest blue and red supergiant stars in nearby galaxies as a distance indicator. This work culminated in a series of papers by A. Sandage, R. Humphreys and others in the 1970–80’s on the bright stellar content of galaxies in the Local Group and in a handful of more distant late-type spirals (see reviews by [70], [31] and, more recently, [68]). While the brightest red supergiants were soon recognized as a more accurate secondary standard, thanks to the smaller dependence of their brightness on the parent galaxy luminosity, here I will briefly summarize the work concerning the brightest blue stars, generally of types from late B to A. Note that a photometric color selection criterion  $(B - V)_0 < 0.4$  isolates supergiants of spectral type earlier than F5. Even if nowadays this method is not considered sufficiently accurate when compared with the best available extragalactic distance indicators, it has been adopted also during the past decade whenever observational material on more accurate distance indicators (Cepheids, TRGB, SN Ia, etc.) was lacking.

Some of the main difficulties in using the luminosity of the brightest stars in galaxies as a standard candle were recognized by Hubble himself, namely the unavoidable confusion between real ‘isolated’ stars and unresolved small stellar clusters or H II regions, and the presence of foreground objects in the Galaxy. While the latter problem is easily solved by avoiding stars of intermediate color in the c-m diagram, the former is much more subtle, eventually becoming the main criticism to the bright blue star method raised by Humphreys and collaborators [33], [32], who, with stellar spectroscopy in some of the nearest galaxies, revealed the composite nature of many of those objects which were previously considered to be the brightest stars.

Hubble’s original calibration of the mean absolute magnitude of the three brightest stars in a galaxy,  $M_B(3)_0$ , introduced as a more robust measure of the visually most luminous stars than the single brightest star, was flawed (he adopted  $\langle M_{pg} \rangle \simeq -6.3$ , about 3 magnitudes too faint), which was partly responsible for the large value he found for the expansion rate of the universe.

The dependence of  $M_B(3)_0$  on the parent galaxy luminosity [ $M_B(3)_0 \propto M(\text{gal})_0$ ], an effect already discussed by Hubble and by Holmberg, was first investigated in detail by [71] as part of a series of papers on the brightest stars in resolved spiral and irregular

galaxies, with distances calibrated via observations of Cepheids (see [69], and references therein). The existence of such a correlation hampers the use of the luminosity of the brightest blue stars as a standard candle. Moreover, the standard deviation of a single observation as measured by [71] was  $\simeq 0.5$  mag, much larger than their quoted 0.1 mag for the standard deviation of the mean of the three brightest red supergiants. The latter were later also found to obey a dependence on the parent galaxy luminosity, albeit with a shallower slope.

The  $M_B(3)_0 - M(\text{gal})_0$  relationship has been customarily interpreted as a statistical effect, since more luminous and larger galaxies can populate the stellar luminosity function up to brighter magnitudes than smaller galaxies. A flattening of this relation might be detected in galaxies brighter than  $M(\text{gal})_0 = -19$  [70], corresponding to the total luminosity of large spirals, in which the observed limit is simply imposed by the luminosity of the brightest post-main sequence B- and A-type stars in the H-R diagram. Therefore, while large, late-type spiral galaxies, such as M101, may contain stars as bright as  $M_B \simeq -10$ , the brightest blue stars in dwarfs like NGC 6822 or IC 1613 are found at  $M_B \simeq -7$ . Numerical simulations by [73] and [25] have provided support for the statistical interpretation, making variations in the stellar luminosity and mass function among galaxies unnecessary to explain the observed trend.

Among the most recent compilations of the brightest blue stars in nearby resolved galaxies is that of [24], based on updated stellar photometry of galaxies included in previous works by [59], [38] and [68]. The resulting relation between  $M_B(3)_0$  and parent galaxy total luminosity is shown in Fig. 2, where different symbols are used for 17 *standard* galaxies and a few *test* galaxies (only those with available Cepheid distances from the list of [24] are shown, together with IC 4182 [69]). In this plot, distances for some of the galaxies have been updated from the results of the HST Key Project, as summarized by [20] (as an aside, no systematic study of the brightest stars in the whole sample analyzed by the Key Project has been published). The standard galaxies define a linear regression:

$$M_B(3)_0 = -1.76 (\pm 0.45) + [0.40 (\pm 0.03)] M_B(\text{gal})_0 \quad (1)$$

with a standard deviation  $\sigma(M_B) = 0.26$ . The rather small dispersion is, at least partly, a result of the particular selection of the ‘standard’ galaxies made by [24]. In fact,  $\sigma(M_B) \simeq 0.6$  is obtained from the data of [59] and [68]. Differences in the treatment of foreground and internal extinction exist between different authors. Furthermore, [70] has advocated the use of the irregular blue variables among the brightest blue stars, a view strongly opposed by [33]. We must also note that consensus still has to be reached concerning the choice of the individual brightest blue stars in the most luminous galaxies in Fig. 2. For example, spectroscopy of bright objects in M81 by [96] has revealed that none of the seven brightest supergiant candidates could be confirmed as a single star, imposing a fainter upper limit for  $M_B(3)_0$ . The points in Fig. 2 corresponding to the other luminous galaxies, M31 and M101, are likely to be affected by similar problems, and could therefore also be revised to lower  $M_B(3)_0$  values.

Numerical simulations such as those by [73], shown by the dotted (50 % limits of the probability distribution) and long-dashed (99.5 %) curves, can explain both the trend, which however is predicted not to be linear, and the dispersion in the observational data,

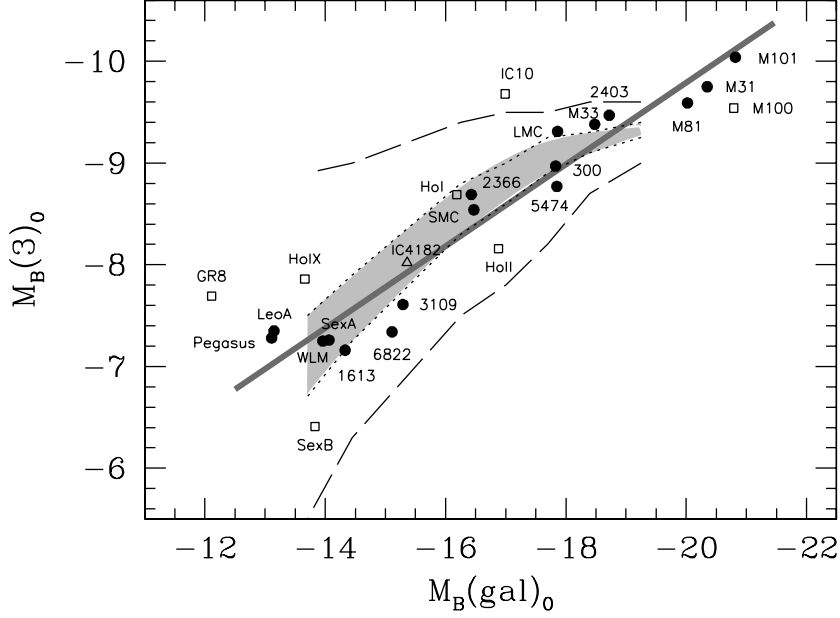


**Fig. 2.** The relationship between the average magnitude of the three brightest blue stars and the magnitude of the parent galaxy. Data from [24], with minor updates on the distances. Full dots refer to the calibration galaxies, while the open symbols are used for the additional test galaxies for which a Cepheid distance is available. The straight line represents the linear regression to the calibration points. The numerical simulations showing the 50 % and 99.5 % limits of the probability distribution (*dotted* and *long-dashed* lines, respectively) are from [73]

at least up to the maximum galaxy brightness considered in the models. It appears that removing objects with Cepheid distances from the linear regression as done by [24] (those shown here by the open symbols) might not be fully justified, since a considerable dispersion at the low-luminosity end is expected from the incomplete filling of the stellar luminosity function. However, considerations on the evolutionary status of some of the dwarf galaxies might provide some justification for the removal of some of the data points.

The general conclusion we can draw from these results is that distance moduli to individual galaxies cannot be determined from the simple photometry of bright blue stars to better than at least 0.5 mag (0.9 mag according to [68]). This is larger than  $\sigma(M_B)$ , as a result of the strong dependence of  $M_B(3)_0$  on  $M(\text{gal})_0$ . Moreover, the necessity of spectroscopic confirmation of the brightest stars must be stressed. Outside of the Local Group, after the initial efforts at moderate resolution in M81, NGC 2403, M101 [32], [96], high-quality spectroscopy of the bright stellar content of galaxies has come within reach of modern equipment on 8m-class telescopes at increasing distances. As an example, I cite the work by [8] and [9] in NGC 3621 and NGC 300, which will be discussed later in this paper.

To conclude the section on extragalactic distances based on the luminosity of the brightest blue stars, a handful of works published in the last decade can be highlighted:

- *brightest stars in galaxies with radial velocities  $< 500 \text{ km s}^{-1}$* : a project aiming at the measurement of the distance of a large number of (mostly dwarf) resolved galaxies in the Local Volume ( $v_{\text{rad}} < 500 \text{ km s}^{-1}$ ) has been carried out since 1994 by Karachentsev and collaborators, using a  $M_B(3)_0$  calibration obtained by [38] (see [75], [16] and references therein). Recently the TRGB method is being used [39].
- *brightest stars in Virgo galaxies*: brightest star candidates have been detected from ground-based images taken under excellent seeing conditions in two Virgo spirals, NGC 4523 [74] and NGC 4571 [57]. Distances of  $13 (\pm 2)$  and  $14.9 (\pm 1.5)$  Mpc were derived, respectively, from yellow and blue supergiants. The brightest stars in a third galaxy in Virgo, M100, were discussed by [21], based on HST WFPC2 images. The Cepheid distance from the HST Key Project is  $14.3 (\pm 0.5)$  Mpc.
- *additional galaxies in the field ( $D \sim 7\text{--}8 \text{ Mpc}$ )*: the brightest blue and red supergiants have been used by [77], [78] and [79] to measure distances to a few spiral galaxies, including NGC 925 and NGC 628, adopting the calibration of [68].

### 3 Spectroscopic Diagnostics: Equivalent Width of the Balmer Lines

The spectroscopic approach alleviates the major difficulties of the photometric method described in the previous section. Small clusters, close companions and H II regions can be easily identified from line profiles, composite appearance of the spectrum and presence of nebular lines. In addition, the analysis of the spectral diagnostics (equivalent widths, line profiles, continuum fluxes) can provide detailed information on element abundances, spectral energy distributions, wind outflows and stellar reddening.

The discovery of a relationship between stellar optical spectral lines and luminosity dates back to the 1920's, when the character of the lines, diffuse vs. sharp, and their strength were found to correlate with the absolute magnitude of stars of type A and B [1], [2], [17], [93]. The hydrogen Balmer lines in particular were soon recognized to play an important role in connection with the problem of measuring stellar luminosities using spectra, a fact which continues to hold true even for the most recent techniques involving the spectral analysis of blue supergiants. The luminosity effect on the width of the Balmer lines derives from their dependence on the pressure (Stark broadening), as realized by [30] and [80], with a line absorption coefficient in the wings proportional to the electron pressure (and also dependent on the temperature). As a result, narrower and weaker lines are formed with decreasing pressure and surface gravity, and consequently with increasing luminosity.

I will not discuss here additional, somewhat related methods, including: *i*) the relationship between  $M_V$  and the strength of the O I triplet at  $\lambda \sim 7774 \text{ \AA}$ , which holds for the A–G spectral types [4]; *ii*) the strength and the effective wavelength of the Balmer jump, as in the Barbier, Chalonge & Divan classification system [12], and *iii*) photometric indexes centred on selected Balmer lines, such as the  $\beta$  index used by [14], [15] and [95]. Another luminosity diagnostic for B9–A2 supergiants, the strength of

the Si II  $\lambda\lambda$  6347, 6371 lines, was proposed by [66], but [19] showed that this indicator breaks down for bright SMC stars, as a likely effect of the reduced metallicity.

Work by [56] on the equivalent width of the H $\gamma$  line,  $W(H\gamma)$ , led to a calibration of its relationship with absolute magnitude, lower values of  $W(H\gamma)$  being found for high-luminosity stars. A spectral type dependence among the B and A stars of different luminosity classes was also detected. The cut-off at the bright end of this early calibration ( $M_V > -7$ ) was imposed by the scarcity of supergiant stars with known distances.

Refinements to the calibration of this technique were introduced by [7] and by [37]. The latter used a  $W(H\gamma)-M_V$  calibration based on Galactic stars to estimate the distance to the Magellanic Clouds, thus pioneering stellar spectroscopy as a way to determine extragalactic distances (see also [13]). More recent calibrations have been proposed by [54] (O–A dwarfs and giants), [92] and [28] (supergiants), accounting for the spectral type dependence. Among the applications, I recall the work by [5], who used  $W(H\gamma)$  to determine luminosity classes for a large number of stars in the SMC.

Correlations between Balmer lines of blue supergiants and stellar luminosity are not restricted to the use of H $\gamma$ . A strong luminosity effect on the H $\alpha$  line was found from narrow-band photometry of Galactic early-type stars by [3]. Later [82] turned their attention to the equivalent width of the H $\alpha$  and H $\beta$  lines in a sample of B–A supergiants in the LMC and SMC. The availability in these extragalactic systems of a large number of blue supergiants up to extreme luminosities, all at a common distance and with small reddening, is a major advantage for calibration purposes. The H $\alpha$  and H $\beta$  lines are in emission for the visually brightest blue stars in the Clouds, as recognized since the early stellar spectroscopic work in these galaxies [18], a signature of the presence of extended atmospheres and mass loss through stellar winds. The luminosity effect is particularly strong in H $\alpha$ , which in late-B and early-A supergiants begins to show a clear emission nature, mostly with a characteristic P-Cygni profile, around  $M_V = -7$  [65]. The filling of the line profiles by stellar wind becomes progressively smaller as one proceeds to Balmer lines of higher order, so that H $\gamma$ , H $\delta$ , etc. are increasingly better diagnostics of stellar surface gravity. Examples of H $\alpha$ , H $\beta$  and H $\gamma$  line profiles are shown in Fig. 3 for stars of different visual brightness, from  $M_V = -9.3$  to  $-6.2$  in the LMC (the two brightest objects), the Milky Way (HD 92207) and NGC 300 (the three fainter objects), all plotted at the same intermediate spectral resolution. Excellent examples of higher resolution profiles of Balmer lines of B–A supergiants can be found in the papers by [65], [40] and [89].

For extragalactic distance studies it is essential that the scatter in the relationships between observables be small. In the case of the equivalent width of H $\alpha$  and H $\beta$  vs. magnitude, the rms scatter found by [82] for about 40 B5–A0 supergiants in the LMC was 0.3–0.4 mag. However, the scatter doubles for similar stars in the SMC, an effect attributed to a metallicity dependence of the mass loss rate. When H $\gamma$  and H $\delta$  are considered [83] a  $\sim 0.5$  mag dispersion is found in the LMC. On the other hand, [92] and [28], using their  $W(H\gamma)-M_V$  calibration, claim a probable error  $\simeq 0.2$  mag (standard deviation  $\simeq 0.3$  mag), for a single observation. However, we note that in the latter two works stars brighter than  $M_V = -8$  are excluded from the calibration, somewhat reducing its usefulness for extragalactic work.



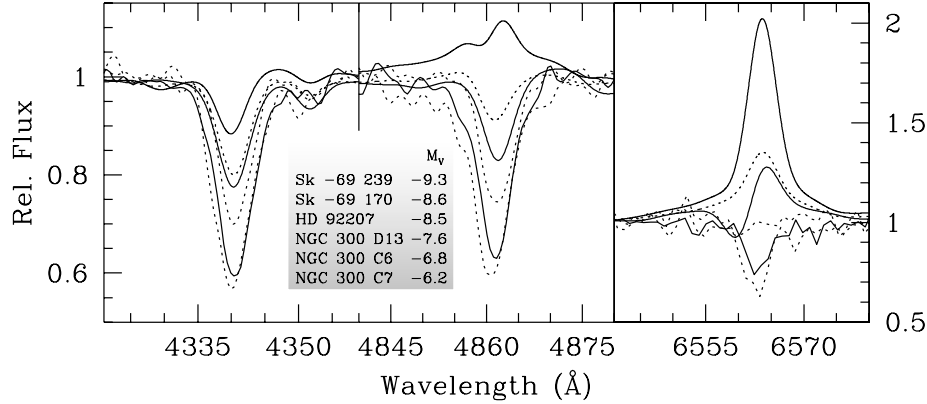


**Fig. 3.** Examples of  $H\gamma$  (left),  $H\beta$  (middle) and  $H\alpha$  (right) line profiles in blue supergiants of different visual brightness (decreasing from top to bottom, as indicated in the legend) in the LMC, Milky Way and NGC 300. The LMC and Galactic spectra (courtesy N. Przybilla and R. Kudritzki) have been degraded to the 5 Å resolution of the NGC 300 data

Since the mid-1980's not much work has been published about new applications of the  $W(H\gamma)-M_V$  relationship, possibly because of the somewhat uncertain results obtained in the Clouds and, most of all, because of the lack of high-quality spectra for blue supergiants in galaxies beyond the Magellanic Clouds. With the availability of 8–10m telescopes in recent times the spectroscopy of a large number of stars well beyond the Local Group boundaries has become feasible, and new calibrations and tests of spectroscopic luminosity diagnostics are likely to appear in future years. Several projects are underway within our group and others to use the current generation of multi-object spectrographs (FLAMES, FORS and VIMOS at the VLT, DEIMOS at Keck, GMOS at Gemini) to observe a large fraction of the bright stellar content in galaxies of the Local Group and beyond.

A first, modern version of the  $W(H\gamma)-M_V$  relation for B and A supergiants, based on CCD spectra collected within our group, is reproduced in Fig. 4. The sample shown contains objects from the following galaxies: NGC 300 [9], Milky Way [40], LMC and SMC [60], M33 and M31 [50], [51]. It has been subdivided, somewhat arbitrarily, into three separate classes according to the stellar spectral type range: early B (B0–B4, full symbols), B8–A0 (open symbols) and A1–A9 (crosses).

The slope of the empirical relationship in Fig. 4 becomes shallower for the later spectral types, as indicated by the regressions corresponding to the B8–A0 (dashed line) and A1–A9 (dotted line) classes. This trend with spectral type is well-known from previous work, with a maximum  $W(H\gamma)$  at a given  $M_V$  around type F0 for supergiants [37]. Contrary to the calibration by [28], the new diagram is populated up to very bright magnitudes,  $M_V \simeq -9$ . The relationship defined by the B8–A0 subgroup is rather tight, with a standard deviation of about 0.3 mag (bottom panel of Fig. 4), and is given by

$$M_V = -9.56 (\pm 0.15) + [1.01 (\pm 0.07)] W(H\gamma) . \quad (2)$$

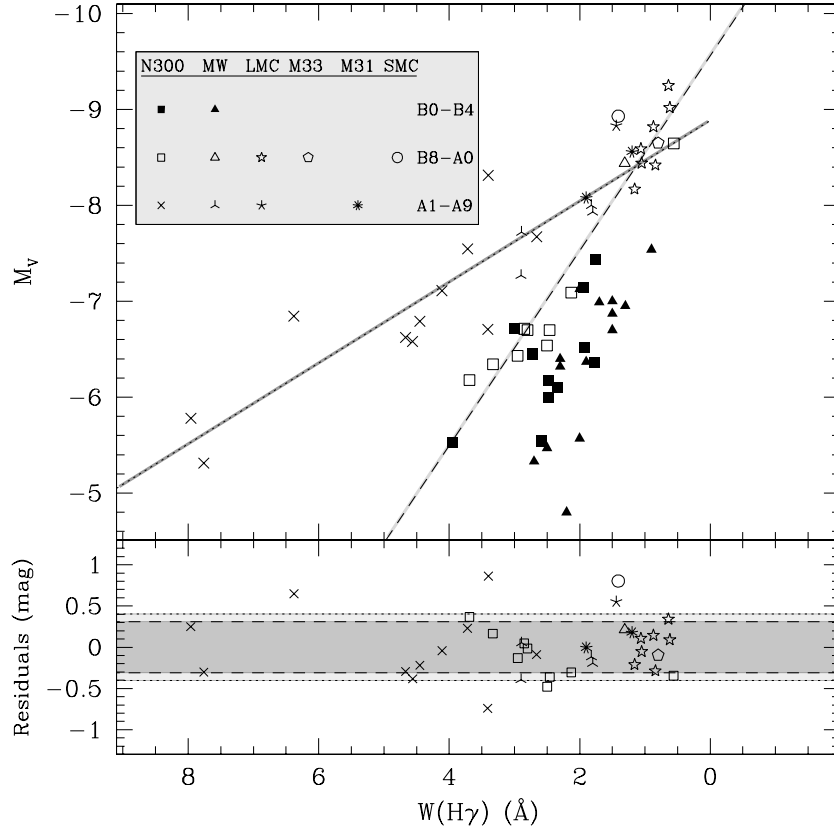


**Fig. 4.** (Top) The  $W(H\gamma)$ – $M_V$  relationship for B–A supergiants in NGC 300, Milky Way, Magellanic Clouds, M31 and M33. The sample has been divided into three classes: B0–B4 (*full symbols*), B8–A0 (*open*) and A1–A9 (*crosses*). The regression lines for the latter two are shown. (Bottom) Residual plot from the regressions for B8–A0 (*open symbols*) and A1–A9 supergiants (*crossed*). The standard deviation is shown by dashed and dotted lines, respectively

The scatter for the later A-type supergiants is 50 % larger. A further subdivision of this broad class might reveal tighter correlations, but currently this is prevented by the small number of objects available. We note the rather large discrepancy of the only A0 Ia supergiant plotted for the SMC (AV 475) from the regression line, with an  $H\gamma$  line too strong for its magnitude. A metallicity effect cannot be excluded at this stage to explain this discrepancy. The measurements of  $W(H\gamma)$  in SMC supergiants by [5], combined with  $M_V$ 's obtained from magnitudes and spectral types in the catalog by [6], are in general agreement with those shown in Fig. 4, although they show a larger scatter. This might be, at least partly, related to the necessity of redefining the spectral type classification at low metallicity, as shown by [47].

To conclude, by restricting the analysis to a narrow range in spectral types (B8 to A0) the scatter about the mean  $W(H\gamma)$ – $M_V$  relation is on the order of 0.3 mag, which

makes this spectroscopic technique rather appealing for its simplicity and accuracy, at least for metallicities comparable to that of the LMC and larger, whenever moderate resolution spectra of a sufficient number of B8–A0 supergiants in a given galaxy are available. Additional tests at lower metallicity (for example in the SMC) should be carried out to verify the dependence on chemical abundance.

## 4 The Wind Momentum–Luminosity Relationship

The discovery and empirical verification of a relationship between the intensity of the stellar wind momentum and the luminosity of massive stars is certainly one of the foremost successes of the theory of line driven winds, which is presented in R. Kudritzki’s contribution in this volume (see also [42] for a review). The predicted Wind Momentum–Luminosity Relationship (WLR) can be written as:

$$\log D_{mom} = \log D_0 + x \log \frac{L}{L_\odot} \quad (3)$$

where the linear regression coefficients  $D_0$  and  $x$  are derived empirically from observations of O, B and A stars at known distances. The modified wind momentum  $D_{mom} = \dot{M} v_\infty (R/R_\odot)^{0.5}$ , i.e. the product of the mass-loss rate, wind terminal velocity and square root of stellar radius, is determined spectroscopically, once the magnitude of the star is measured. A spectral type dependence is found, as shown in Fig. 5, as a result of the different ionic species driving the wind at different stellar temperatures. In fact the slope  $x$  corresponds to the reciprocal of the exponent  $\alpha'$  of the power-law describing the line-strength distribution function. The predicted value lies around  $\alpha' = 1/x = 0.6$ . The effects of metallicity  $Z$  are also to be empirically verified, while the predictions for the dependence of both  $\dot{M}$  and  $v_\infty$  indicate that approximately  $D_{mom} \propto Z^{0.8}$  [91].

Since all massive and luminous blue stars show signs of mass loss, it is interesting to take advantage of this through the WLR as a way to measure extragalactic distances. In practice, one needs to obtain the mass-loss rate from the  $H\alpha$  line fitting, and the photospheric parameters (temperature, gravity and chemical composition) from optical absorption lines in the blue optical spectral region (4000–5000 Å). An empirically calibrated WLR as a function of metallicity would then allow the determination of distances, once the apparent magnitude, reddening and extinction are known. The latter quantities can be derived from the observed spectral energy distribution and theoretical models calculated with the appropriate photospheric parameters. The method is backed by a strong theoretical framework, especially for the hot O stars, which allows us to deal quantitatively with the spectral diagnostics of blue supergiants. However, its observational application requires careful spectroscopic analysis and modeling, which can make it intimidating at first. On the other hand, the same analysis provides us with a large amount of information on the physics of massive stars. Here I will briefly summarize the results obtained so far concerning the calibration of the WLR, by discussing the O stars separately from the B–A supergiants, referring the reader to the papers cited above for the theoretical aspects and for details on how the stellar and wind parameters are extracted from the observational data.

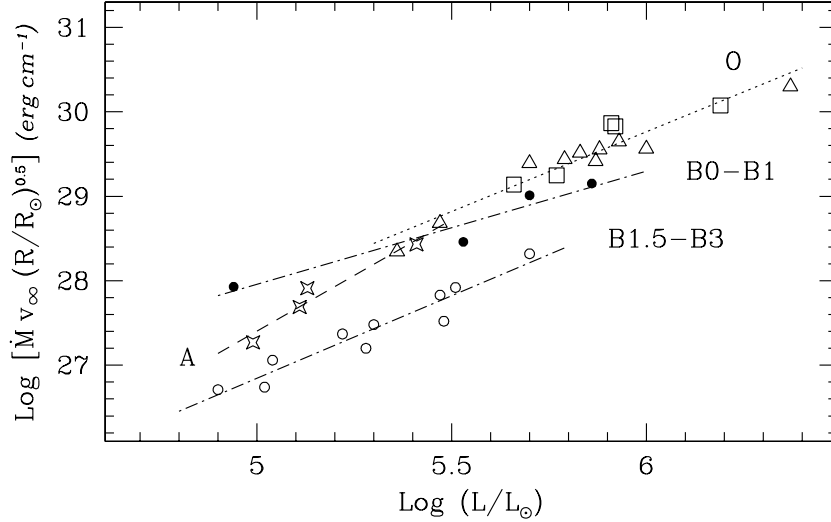


**Fig. 5.** Spectral type dependence of the WLR for Galactic supergiant stars. Different symbols are used for the different spectral type ranges, and regression lines are drawn. Adapted from [40], with data from the same paper. For O stars the blanketed model results of [64] and [27] have been used

#### 4.1 O Stars

For O stars the reference work remains the paper by Puls et al. [63], in which theoretical results from unified model atmosphere calculations were used to measure mass-loss rates from  $H\alpha$  line profiles. Their method overcomes the inaccuracies related to the use of the equivalent width of the  $H\alpha$  line from the wind emission, corrected for photospheric contribution, as done by [46] and [44]. For a sample of Galactic and Magellanic Clouds stars the relevant parameters were measured from spectra in the UV ( $v_{\infty}$ , based on the P-Cygni profiles of strong resonance lines) and in the optical ( $T_{eff}$ ,  $\log g$ ), and from the analysis of the  $H\alpha$  line profile ( $\dot{M}$ , wind velocity law). Separate relations were found by Puls and collaborators for different luminosity classes, the supergiants having larger wind momenta than giants and dwarfs at a given luminosity. Moreover, reduced wind momenta were measured in the Magellanic Clouds when compared with the Milky Way stars, as a manifestation of a metallicity effect on the strength of the wind. More recently, [27] have determined the WLR for O stars in a single Galactic association, Cyg OB2, thus reducing the uncertainty in stellar distances as a source of scatter in the calibration. Recent improvements in the stellar models allowed these authors to account for the effects of line blocking and blanketing from metals. As explained by [64] the consequent cooler temperature scale for O stars, when compared with  $T_{eff}$  calibrations based on unblanketed atmospheres, modifies the WLR significantly, leading in particular to an indication that the luminosity class dependence might be no longer present, in agreement with the theoretical predictions by [90], but instead that wind clumping might mimic higher mass-loss rates in the more extreme cases, affecting preferentially

stars with an  $H\alpha$  profile in emission. Fig. 6 illustrates these results, where the Galactic sample of [64] and the Cyg OB2 stars of [27] have been divided according to the nature of the  $H\alpha$  line profile, i.e. in emission (open symbols) or in absorption partly filled by wind emission (full symbols). The resulting tight relations are clearly displaced from one another by about 0.3 dex, with the less extreme objects ( $H\alpha$  in absorption, optically thin winds) lying very close to the theoretical relationship defined by [90]. The hypothesis of clumping to explain the apparently higher mass-loss rates in stars with  $H\alpha$  in emission is very appealing, but requires further observational confirmation, with the UV-to-IR spectral analysis of a large number of O stars.

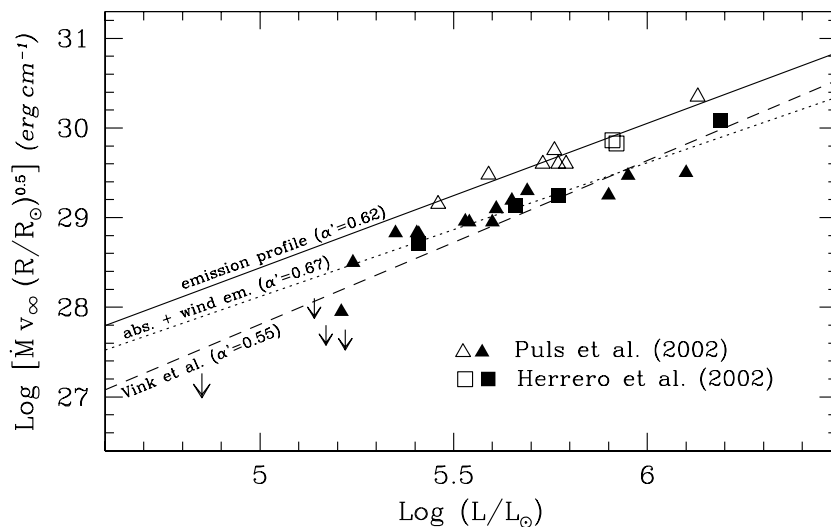


**Fig. 6.** The WLR for Galactic O stars, with data from [64] and [27]. The O star sample has been subdivided according to the character of the  $H\alpha$  profile, either in emission (*open symbols*) or in absorption partly filled by wind emission (*full symbols*). The linear fits to the two sub-samples are shown, together with the theoretical models by [90]. The slope of the line strength distribution function  $\alpha' = 1/x$  is indicated for each regression

## 4.2 B and A Supergiants

Even if the WLR calibration for the O stars is probably the best available to date, and the one upon which most observational and theoretical work has been concentrated, it is the late-B and the A supergiants which offer the largest potential as extragalactic distance indicators. In fact, these stars are in general much less affected by crowding and confusion problems, which afflict O stars, normally found in OB associations and/or within H II region complexes. Besides, they attain brighter magnitudes in the optical ( $M_V \simeq -9$  for A hypergiants, vs.  $M_V \simeq -7$  for the brightest O Ia stars), as the result of a combination of stellar evolution across the upper H-R diagram at roughly constant

luminosity and smaller bolometric corrections in the covered temperature range ( $T_{\text{eff}} \simeq 13000 - 7500 \text{ K}$ ). Their extreme luminosities make their analysis less affected by the presence of fainter companions, which can be, if bright enough to be of importance, detected by their spectral signatures. As a downside, a large fraction of the brightest supergiants are photometrically variables at the 0.1–0.2 mag level [86], [26], and this should be taken into account when trying to use them as distance indicators.

With the modern spectroscopic capabilities at 8m-class telescopes, A-type supergiants should be within reach of a quantitative analysis out to distance moduli ( $m - M$ )  $\simeq 30$ –31, i.e. out to the distance of the Virgo Cluster. A great amount of work, however, still needs to be done regarding the identification of suitable targets on one hand, and the calibration of the WLR on the other.

**Selecting the Candidates** For those resolved galaxies where extensive stellar classification work has not already been carried out, which in practice, with a few exceptions, means all galaxies outside of the Local Group, as well as a considerable fraction of Local Group members, spectral types of blue supergiant candidates must be found from scratch, overall a rather lengthy process. This is accomplished by first obtaining stellar photometry in two or more bands, typically  $B$  and  $V$ , from CCD images, and subsequently concentrating the spectroscopic follow-up on those isolated objects in the color and magnitude range expected for blue supergiants. We have found it very helpful, if not necessary, to obtain also narrow-band  $H\alpha$  images, to limit as much as possible the contamination on the final stellar spectra from nebular lines. This is particularly true in the late-type, star-forming galaxies which are the natural targets for the application of the WLR. The availability of large-format CCD mosaics at several 2–4 meter telescopes around the globe, covering as much as half a degree or more on the sky in a single exposure, is making the photometric surveys required for target selection time-efficient even when considering a large number of nearby galaxies.

The photometric selection is always affected at some level by the presence of ‘intruders’ in the c-m diagram (unresolved stellar groups, unidentified small H II regions, stars with greatly different extinction, and more exotic objects), and can be verified only *a posteriori*, once the spectroscopy has been carried out. This is becoming less of a problem, with the availability of multiobject spectrographs, like FLAMES at the VLT, which allow the simultaneous observation of hundreds of spectra.

As an example of some recent results, Fig. 7 shows the c-m diagram of the Sculptor Group galaxy NGC 300, obtained from 2.2m/WFI CCD images at La Silla by W. Gieren, where the objects we have studied spectroscopically with FORS1 at the VLT have been indicated [9]. With our original selection criterion ( $-0.3 < B - V < 0.3$ ,  $V < 21.5$ ) we intended to isolate late-B and early-A supergiants. The confirmed stellar types, from B0 to F2, correspond rather well with the expected location in the c-m diagram. The few pre-selected H II regions have rather blue  $B - V$  colors, while some objects characterized by a composite spectrum are found at faint magnitudes. More interesting interlopers are a foreground Galactic white dwarf and a WN11 emission line star, the latter analyzed by [10]. The high success rate in the case of NGC 300 has been made possible by the careful analysis of the broad-band and  $H\alpha$  images, in combination with the modest distance (2 Mpc), and likely by the small foreground+internal

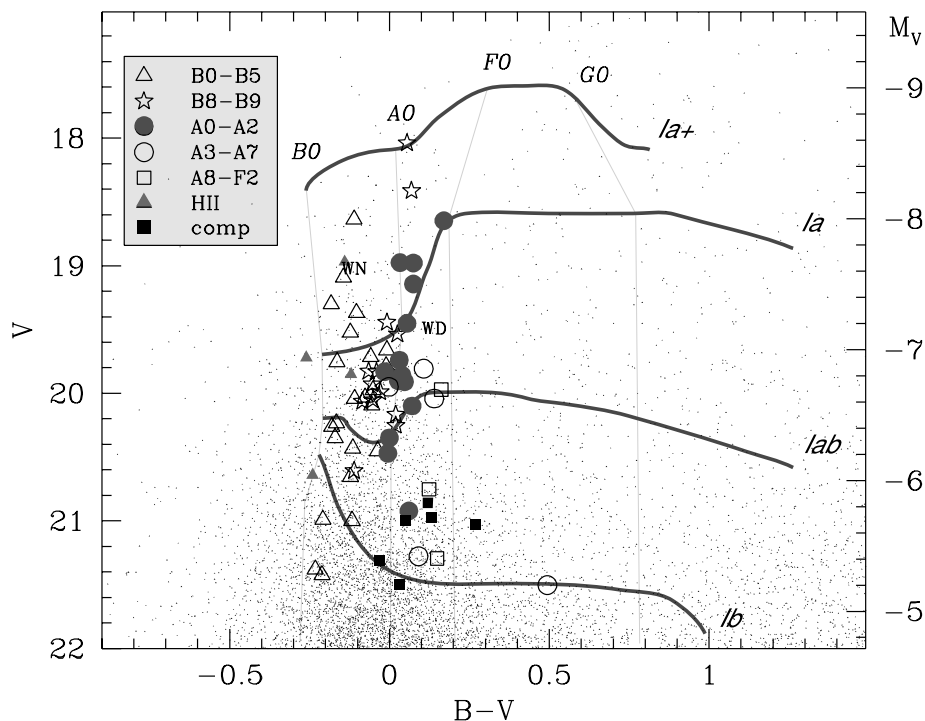


**Fig. 7.** Color-magnitude diagram of NGC 300. The supergiants studied spectroscopically by [9] have been divided into separate ranges of spectral type, according to the legend in the upper left. Observed H II regions and objects with composite spectra are also indicated, together with the locations of a foreground white dwarf (WD) and a WN11 star (WN). The magnitude-color calibration for  $Ia^+$ ,  $Ia$ ,  $Iab$  and  $Ib$  stars is the same as in Fig. 1

reddening, even though a number of bright supergiants were found to be contaminated by nebular emission in subsequent  $H\alpha$  spectra used for the mass-loss determination. Work similar to the one described for NGC 300 has been carried out at the VLT by our group in two additional galaxies, NGC 3621 [8] and a second galaxy in Sculptor, NGC 7793 (work in preparation). We are also securing wide-field images of about a dozen nearby ( $D < 7$  Mpc) galaxies from La Silla and Mauna Kea, as well as obtaining HST/ACS imaging of selected fields in NGC 300, NGC 3621 and M101 for accurate stellar photometry of confirmed and candidate blue supergiants.

**Calibration of the WLR** The current calibration of the WLR for Galactic A-type supergiants, given by [40], rests on only four stars, because of the difficulty to measure reliable distances and reddening corrections for this type of objects when located in the Milky Way. In their paper, 14 early B supergiants were also studied, but I will not include them in the following discussion because of their somewhat lower appeal (being fainter) for extragalactic distances work. Apparently they also do not conform to the

same relationship as the A supergiants, as seen in Fig. 5. A subset of these stars (those in the B1.5–B3 spectral type range) were found to have low wind momenta when compared to the O and early B stars, an anomaly which is not currently understood within the theoretical framework. I simply mention here that several observing programs are underway on the early B supergiants in Local Group galaxies, utilizing optical spectroscopy to derive photospheric parameters and abundances [76], [81] and UV spectroscopy to measure wind velocities [84], [11], in order to obtain a better understanding of their wind properties.

From the paucity of Galactic calibrators it is clear that the sample must be enlarged by observing additional bright B–A supergiants in nearby galaxies, before any attempt to measure independent distances with the WLR is made. The first high resolution spectra of A supergiants in M33 and M31, two in each galaxy, have been obtained with the Keck telescope by [50] and [51], respectively, demonstrating that, at least at distances smaller than 1 Mpc, all stellar wind parameters ( $\dot{M}$ ,  $v_\infty$  and the exponent  $\beta$  of the wind velocity law) can be satisfactorily obtained from fitting the  $H\alpha$  line profile. The paper on the M31 stars, in particular, shows several examples of how varying the wind parameters influences the calculated profiles. The wind analysis from the  $H\alpha$  line must still be carried out in a larger number of supergiants in these two galaxies, however. The M33 spiral, in particular, appears to be an ideal target, because of its moderate distance and its favorable inclination on the plane of the sky. The radial chemical abundance gradient in this galaxy is such that it will allow the investigation of the metallicity effect on the WLR. We are currently planning to secure spectra at the required resolution (about 1–2 Å) with Keck equipped with the new multiobject spectrograph DEIMOS.

In 1999 we have started to use the FORS spectrograph at the VLT in order to increase the sample of extragalactic A-type supergiants having a spectroscopic coverage. Two are the principle goals: to determine stellar abundances, which are important for galactic and stellar evolution investigations, and to measure wind momenta, for an experimental verification and calibration of the WLR. The very first targets, a handful of blue supergiants in NGC 6822, were observed during the commissioning phase of FORS1, confirming that even at relatively low resolution (5 Å) quantitative spectroscopy can be successfully carried out, with regard to both stellar metallicities and mass-loss rates [55]. An important step was taken with the subsequent analysis of stellar spectra in NGC 3621 [8], so far the most distant galaxy, at  $D \simeq 6.7$  Mpc, for which spectroscopy of individual supergiants has been published. Unfortunately, red spectra covering  $H\alpha$  are still unavailable for this galaxy, so that the mass-loss rate of the blue supergiants discovered could not be determined, except for a highly luminous A1 Ia star ( $M_V = -9.0$ ), for which the wind-affected  $H\beta$  has been used.

After having verified the potential of the available instrumentation, we have turned to more nearby galaxies, NGC 300 and NGC 7793 in the Sculptor Group, combining our project with an investigation of their Cepheid content [58]. While the FORS2 data for NGC 7793 have just recently come in, the analysis of the blue supergiants in NGC 300 has already provided important results concerning the classification and the first A-type supergiant abundance estimates [9], the A-supergiant WLR (in preparation) and the metallicity of the B-type stars [85].



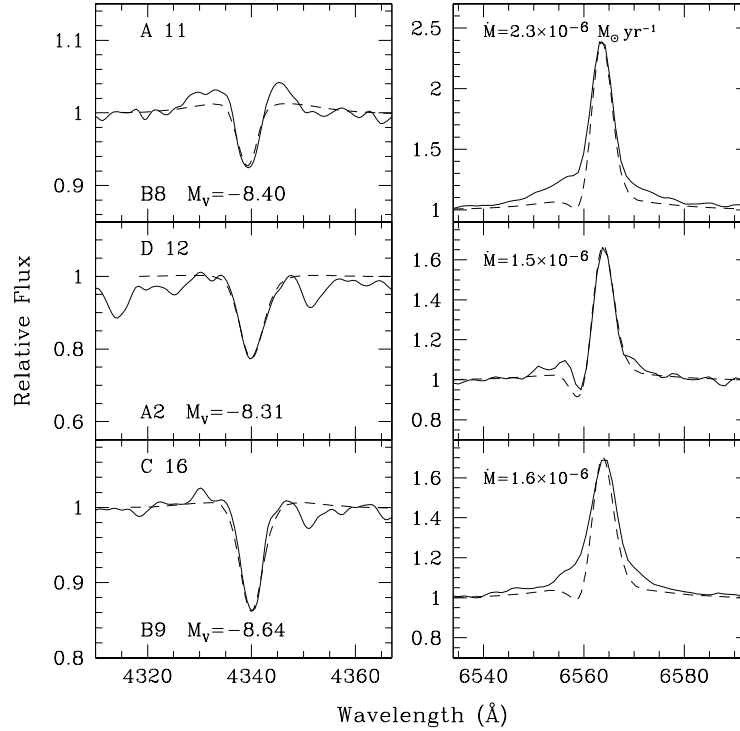


**Fig. 8.**  $H\gamma$  (left) and  $H\alpha$  (right) line profile fits (*dashed lines*) to the spectra of three bright supergiants in NGC 300, obtained with FASTWIND [72]. The identification number from [9] is given in the upper left of each plot. Spectral types and absolute magnitudes are indicated in the lower part of the  $H\gamma$  panels, and mass-loss rates in  $M_{\odot} \text{ yr}^{-1}$  in the  $H\alpha$  panels

The wind analysis has been carried out so far for six A-type supergiants (B8 to A2) from red spectra obtained at the VLT/FORS1 in September 2001. The unblanketed version of the non-LTE line formation code FASTWIND [72] has been used to fit the observed  $H\alpha$  line profiles. The major drawback when using spectroscopic data at moderate resolution is that the terminal velocity cannot be determined from the line fits, forcing us to adopt a reasonable estimate for it,  $v_{\infty} = 150 \text{ km s}^{-1}$ . Although such a velocity is typical for well studied Galactic A supergiants, this assumption is currently the major source of uncertainty in the calculation of the wind momentum in the NGC 300 sample. Fig. 8 illustrates profile fits to  $H\gamma$  (mostly sensitive to gravity) and  $H\alpha$  (mass-loss rate) for three bright A-type supergiants in NGC 300. As can be seen, in some cases we cannot reproduce the observed extended electron scattering wings of  $H\alpha$ , however these features arise in the photosphere, and do not affect the mass-loss rate determination, which is carried out from the peak of the emission. We can also neglect the discrepancies in the blue absorption part of the P-Cygni profiles. This feature is often affected by variability in high luminosity objects, but the corresponding wind momentum variations are contained within the scatter of the WLR [41].

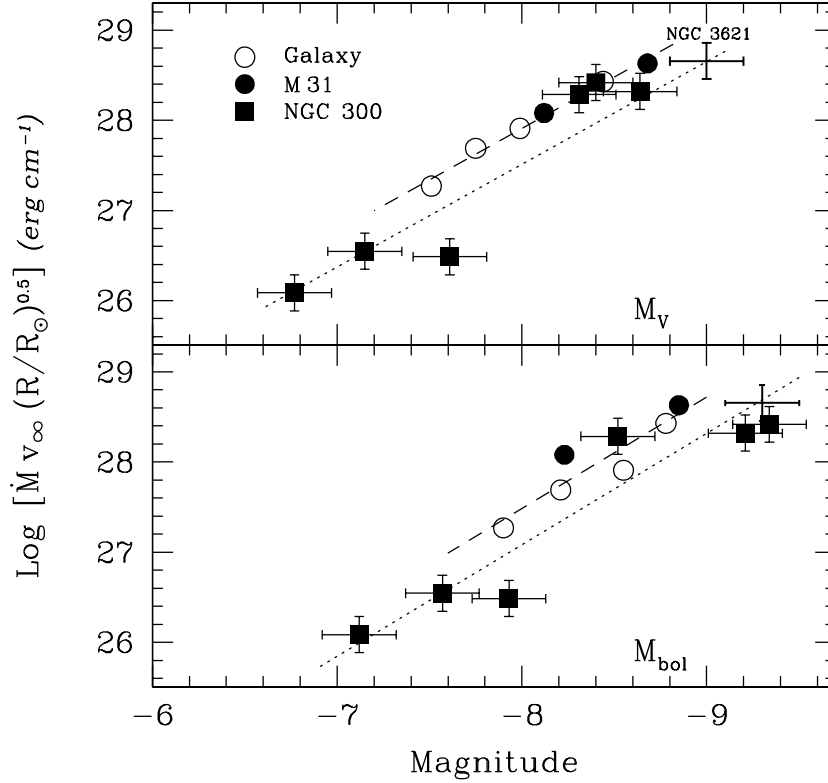


**Fig. 9.** The WLR for A-type supergiants, represented in terms of  $M_V$  (top) and  $M_{bol}$  (bottom). The stellar objects are drawn from samples of blue supergiants in the Milky Way, M31, NGC 300 and NGC 3621. The linear fits to the Galactic and M31 supergiants are given by the dashed lines. A theoretical scaling factor is applied to provide the expected relations at  $0.4 Z_\odot$  (dotted lines)

The WLR determined for the NGC 300 stars analyzed so far, expressed as a relation between modified wind momentum and both  $M_V$  and  $M_{bol}$ , is shown in Fig. 9. The diagrams also include the four Galactic A supergiants studied by [40], the two stars in M31 from [51] and the only star in NGC 3621 for which we were able to determine the mass-loss rate from the  $H\beta$  line (again, assuming here  $v_\infty = 150 \text{ km s}^{-1}$ ).

The metallicity for the NGC 300 stars, which lie all at a similar galactocentric distance, is estimated, from the known H II region oxygen abundance gradient [94] and from the appearance of the stellar spectra, to be around  $0.4 \pm 0.1 Z_\odot$ . The NGC 3621 star has a comparable metallicity. If we adopt an empirical ‘calibration’ of the WLR at solar metallicity as provided by a fit to the Milky Way and M31 points, given by the dashed lines, we can then scale to the lower metallicity using a  $Z^{0.8}$  dependence. This is shown by the dotted lines in Fig. 9.

Let us concentrate on the  $D_{mom} - M_{bol}$  relation, since the sample of objects considered varies in spectral type from B8 to A3, implying different bolometric corrections

by up to 0.7 mag. The corresponding plot in Fig. 9 shows a rather well defined WLR for the Galactic and M31 stars, with a scatter of about 0.2 dex in the modified wind momentum. All the points corresponding to NGC 3621 and NGC 300, except one, agree with the expected approximate location for  $Z = 0.4Z_{\odot}$ . We have yet to carry out the chemical abundance analysis of the discrepant point, and we have currently no obvious explanation for its location in the diagram. Despite this, it appears that even with the moderate resolution spectra at our disposal we can well define the WLR in a galaxy at a distance of 2 Mpc. Of course this result is only preliminary, in the sense that we are still lacking a real calibration of the WLR which we could use to determine extragalactic distances. Analyzing a larger sample of objects, with a range in metallicity from  $Z_{\odot}$  down to  $0.1Z_{\odot}$ , still remains among our top priorities. The obvious candidates for such work are stars in the Magellanic Clouds, and in a number of nearby spirals and irregulars rich in blue supergiants, such as M33, M31 and NGC 6822. Moreover, an improved spectral analysis which takes into account the blanketing and blocking effects of metals in the stellar atmosphere must be carried out.

## 5 A New Spectroscopic Method: the Flux-Weighted Gravity–Luminosity Relationship

A very promising luminosity diagnostic for blue supergiants has been very recently proposed by [43], based on the realization that the fundamental stellar parameters, surface gravity and effective temperature, are predicted to be tightly coupled with the stellar luminosity during the post-main sequence evolution of massive stars. While quickly crossing the upper H–R diagram from the main sequence to the red supergiant phase both the mass and the luminosity of late-B to early-A supergiants remain roughly constant, so that by postulating an approximate mass-luminosity relationship ( $L \sim \mathcal{M}^3$ ) we derive:

$$M_{bol} = a \log(g/T_{eff}^4) + b \quad (4)$$

with  $a \simeq -3.75$ . This equation defines a *Flux-weighted Gravity–Luminosity Relationship* (FGLR), since the quantity  $g/T_{eff}^4$  can be interpreted as the flux-weighted gravity. Even for the most massive stars in the range of interest, 30–40  $\mathcal{M}_{\odot}$ , the mass-loss rate is still small enough that during the typical timescale of this evolutionary phase its effects on the FGLR are negligible, thus justifying our assumption of mass constancy. This is also true, to first order, for the effects of differing metallicities and rotational velocities, as confirmed by the results of evolutionary models [53].

The FGLR is conceptually very simple, and its empirical verification only requires, besides the visual magnitude, the measurement of  $\log g$  and  $T_{eff}$  from the stellar spectrum. A complication arises from the difficulty of measuring these parameters with sufficient accuracy in extremely bright supergiants and hypergiants. Recently, however, sophisticated non-LTE modeling of A supergiants can provide us with tools to determine the stellar parameters with high reliability [88], [61], [62].

As a first test, we have analyzed the spectra of blue supergiants from a number of Local Group galaxies, observed as part of our investigation of the WLR, together with

**Table 2.** Adopted temperature scale for supergiants

Spectral Type	$T_{eff}$
B8	12000
B9	10500
A0	9500
A1	9250
A2	9000
A3	8500
A4	8350

our FORS data on NGC 300 and NGC 3621, as described in Sect. 4. Effective temperatures were estimated from the observed spectral types, according to the correspondence shown in Table 2, except for the lower metallicity objects in SMC, M33 and NGC 6822, for which  $T_{eff}$  was derived from the non-LTE ionization equilibrium of Mg I/II and N I/II. Surface gravities were measured from a simultaneous fit to the higher Balmer lines ( $H\gamma$ ,  $H\delta$ , ...), therefore minimizing the wind emission contamination on the lower-order hydrogen lines. Despite the moderate spectral resolution of the FORS data, which prevents us to fit the wings of the spectral lines, we are able to achieve a similar *internal* accuracy as for the higher resolution spectra by fitting the line cores, about 0.05 dex in  $\log g$ . In practice at low resolution we are fitting the Balmer line equivalent widths to measure stellar gravities, and the FGLR technique is therefore reminiscent of the  $H\gamma$ - $M_V$  relation discussed in Sect. 3. However, we are now considering a larger number of Balmer lines, and including a correction for the temperature dependence through the  $T_{eff}^4$  term. The bolometric correction and the intrinsic color, which allow us to account for reddening and extinction, are also determined from the spectral analysis.

The results are displayed in Fig. 10, where the dashed line is the linear regression:

$$M_{bol} = 3.71 (\pm 0.22) \log(g/T_{eff,4}^4) - 13.49 (\pm 0.31) \quad (5)$$

with a standard deviation  $\sigma = 0.28$  (note that  $T_{eff}$  is expressed in units of  $10^4$  K). This is a very encouraging result for extragalactic work. As can be seen from Fig. 10, the points corresponding to the blue supergiants in NGC 300 define a tight relationship ( $\sigma = 0.20$ ), despite the intermediate resolution of the spectra available. For NGC 3621 the FGLR with just four stars would suggest a distance slightly larger than the assumed Cepheid distance, however the upcoming photometry from HST/ACS is required before we can draw any firm conclusion.

The slope of the empirical FGLR reproduces very well the theoretical expectations from the evolutionary models of [53], while the offset can be interpreted, for example, as a systematic effect on the determination of the stellar parameters, which would not be important in a strictly differential analysis. The apparent increase of the dispersion at high luminosities might be a consequence of the larger role played by stellar rotation and/or metallicity on the flux-weighted gravity. Still, with a standard deviation of 0.3–0.35 mag and with the analysis of about ten blue supergiants in a given galaxy we could be able to determine a mean relationship, and therefore the distance modulus, with an accuracy of  $\sim 0.1$  magnitudes. Our aim is to apply the FGLR method to distances of up

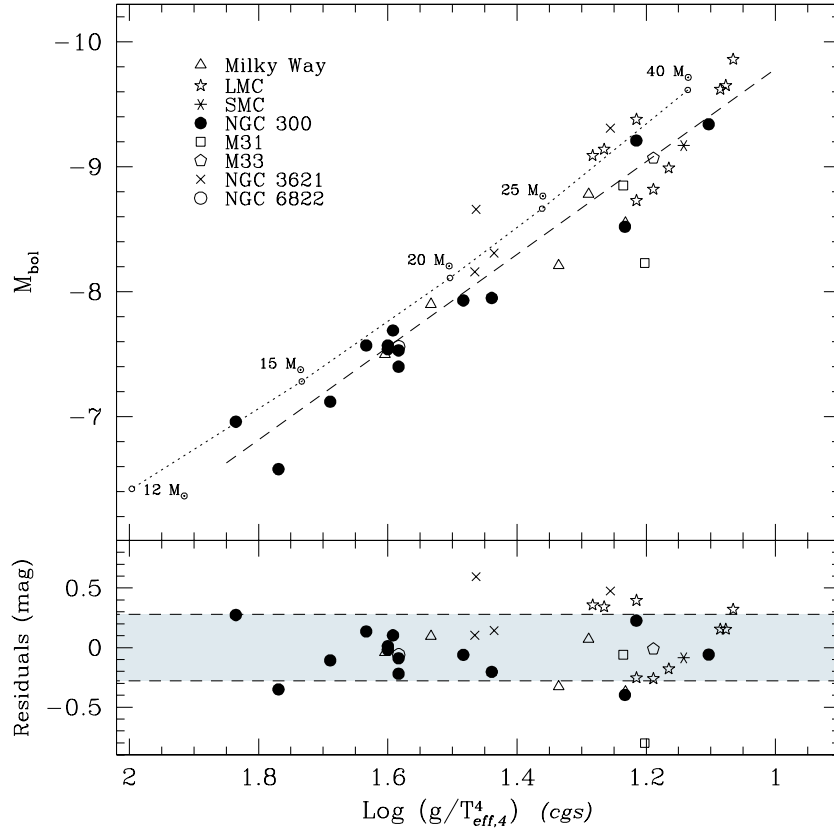


**Fig. 10.** (Top) The relationship between the flux-weighted gravity  $g/T_{eff}^4$  ( $T_{eff}$  in units of  $10^4$  K) and  $M_{bol}$  for B8–A4 supergiants in Local Group galaxies, NGC 300 and NGC 3621. The dashed line represents the linear regression to all the data points. The models at  $T_{eff}=10^4$  K from the evolutionary calculations accounting for rotation ( $v_{in} = 300 \text{ km s}^{-1}$ ) and at solar metallicity of [53] are connected by the dotted line, labeled with the corresponding ZAMS masses. (Bottom) Residuals from the regression shown in the top panel, with the standard deviation indicated by the dashed line

to  $m - M = 30.5$ , where stars brighter than  $M_V = -8$  can be observed with the high-efficiency spectrographs currently available at 8–10m telescopes.

Is the FGLR going to replace the WLR as a more promising distance indicator for blue supergiants? The advantages of the FGLR are multiple. Medium resolution spectra seem to be sufficient, and no red spectrum covering  $H\alpha$  is required, thus reducing the amount of time at the telescope. All the stellar classification work, the chemical abundance analysis and the fit to the higher Balmer lines can be carried out in the blue spectral region, which is also less contaminated by night sky lines. Work on the WLR, however, should continue, especially for early-B stars, for which the assumptions upon which the FGLR rests could fail.

The results shown here are just the starting point in the study of the FGLR. A detailed and extensive calibration work must be carried out in Local Group galaxies, where with instrument like FLAMES (VLT) or DEIMOS (Keck) we can obtain hundreds of blue supergiant spectra. Such observations, besides providing us with an accurate calibration of the FGLR, will also improve our understanding of the effects on stellar evolution of those parameters, like metallicity, mass-loss and angular momentum, which are relevant for a theoretical explanation of the relationship.

As a concluding remark, one may ask the question why we should insist in using spectroscopic methods for blue supergiants, such as the WLR or the FGLR, as extragalactic distance indicators, when other well-tested photometric techniques (e.g. Cepheids and Tip of the Red Giant Branch) promise to obtain perhaps higher accuracy and to reach more distant objects with arguably less observational efforts. The answer is of course that a greater physical insight is gained from the analysis of the stellar spectra, allowing us to determine *for each individual stellar target* the crucial parameters of metallicity and reddening. The discrimination against unresolved companions or small clusters is also possible through the appearance of the spectra. Because of the importance of each of these factors in the application of the main distance indicators used nowadays, possibly leading to some systematic errors in the distance scale if uncorrected for, it is important to continue our efforts to measure a number of ‘spectroscopic’ distances to galaxies of the nearby universe.

## 6 Acknowledgments

I wish to thank the Organizing Committee, W. Gieren and D. Alloin in particular, for inviting me to this workshop and for the hospitality, and R.P. Kudritzki and W. Gieren for their help and encouragement. I am also grateful to N. Przybilla for making his spectra of Magellanic Cloud supergiants available. This research has made use of the SIMBAD database, operated at CDS, Strasbourg, France.

## References

1. W.S. Adams, A.H. Joy: ApJ **56**, 242 (1922)
2. W.S. Adams, A.H. Joy: ApJ **57**, 294 (1923)
3. P.J. Andrews: MNRAS **72**, 35 (1968)
4. A. Arellano Ferro, S. Giridhar, E. Rojo Arellano: Rev. Mex. de Astron. y Astrof., in press (astro-ph/0210695) (2002)
5. M. Azzopardi: A&AS **69**, 421 (1987)
6. M. Azzopardi, J. Vigneau: A&AS **149**, 213 (1982)
7. L. Balona, D. Crampton: MNRAS **166**, 203 (1974)
8. F. Bresolin, R.P. Kudritzki, R. Mendez, N. Przybilla: ApJ **547**, 123 (2001)
9. F. Bresolin, W. Gieren, R.P. Kudritzki, G. Pietrzynski, N. Przybilla.: ApJ **567**, 277 (2002)
10. F. Bresolin, R.P. Kudritzki, F. Najarro, W. Gieren, G. Pietrzynski: ApJ **577**, L107 (2002)
11. F. Bresolin, R.P. Kudritzki, D.J. Lennon, S.J. Smartt, A. Herrero, M. Urbaneja, J. Puls: ApJ, **580**, 213 (2002)
12. D. Chalonge, L. Divan: A&A **23**, 69 (1973)
13. D. Crampton: ApJ **230**, 717 (1979)

14. D.L. Crawford: *AJ* **83**, 48 (1978)
15. D.L. Crawford: *AJ* **84**, 1858 (1979)
16. I.O. Drozdovsky, I.D. Karachentsev: *A&AS* **142**, 425 (2000)
17. D.L. Edwards: *MNRAS* **87**, 365 (1927)
18. M.W. Feast, A.D. Thackeray, A.J. Wesselink: *MNRAS* **121**, 25 (1960)
19. M.W. Feast: *MNRAS* **174**, 9 (1976)
20. W.L. Freedman et al.: *ApJ*, **553**, 47 (2001)
21. W.L. Freedman et al.: *ApJ*, **435**, L31 (1994)
22. C.D. Garmany, P.S. Conti, P. Massey: *AJ*, **93**, 1070 (1990)
23. C.D. Garmany, R.E. Stencel: *A&AS* **94**, 211 (1992)
24. T.B. Georgiev, B.I. Bilkina, N.M. Dencheva: *Astronomy Letters* **23**, 644 (1997)
25. L. Greggio: *A&A* **160**, 111 (1986)
26. G.R. Grieve, B.F. Madore: *ApJS* **62**, 451 (1986)
27. A. Herrero, J. Puls, F. Najarro: *A&A* **396**, 949 (2002)
28. G.M. Hill, G.A.H. Walker, S. Yang: *PASP* **98**, 1186 (1986)
29. E. Hubble: *ApJ* **84**, 158 (1936)
30. E.O. Hulburt: *ApJ* **59**, 204 (1924)
31. R.M. Humphreys: 'The Brightest Stars as Distance Indicators'. In: *The Extragalactic Distance Scale*, ed. by S. van den Bergh, C.J. Pritchett (BYU Press, Provo 1988) pp. 103–112
32. R.M. Humphreys, M. Aaronson: *AJ* **94**, 1156 (1987)
33. R.M. Humphreys, M. Aaronson: *ApJ* **318**, L69 (1987)
34. R.M. Humphreys, C. Blaha, D.B. McElroy: 'Catalog of Luminous Stars in Associations and Clusters'. (Univ. of Minnesota, 1984) unpublished
35. R.M. Humphreys: *ApJS* **39**, 389 (1979)
36. R.M. Humphreys: *ApJS* **38**, 309 (1978)
37. J.B. Hutchings: *MNRAS* **132**, 433 (1966)
38. I.D. Karachentsev, N.A. Tikhonov: *A&A* **286**, 718 (1994)
39. I.D. Karachentsev et al.: *A&A* **389**, 812 (2002)
40. R.P. Kudritzki et al.: *A&A* **350**, 970 (1999)
41. R.P. Kudritzki: 'The Wind Momentum – Luminosity Relationship of Blue Supergiants'. In: *Variable and Non-spherical Stellar Winds in Luminous Hot Stars, Proceedings of the IAU Colloquium No. 169*, ed. by B. Wolf, O. Stahl, A.W. Fullerton (Springer, Berlin, 1999) pp. 405–415
42. R.P. Kudritzki, J. Puls: *ARAA* **38**, 613 (2000)
43. R.P. Kudritzki, F. Bresolin, N. Przybilla: *ApJ* **582**, L83 (2003)
44. H.J.G.L.M. Lamers, C. Leitherer: *ApJ* **412**, 771 (1993)
45. K.R. Lang: *Astrophysical Data* (Springer, New York 1992)
46. C. Leitherer: *ApJ* **326**, 356 (1988)
47. D.J. Lennon: *A&A* **317**, 871 (1997)
48. P. Massey: 'Observations of the Most Luminous Stars in Local Group Galaxies'. In: *Stellar Astrophysics for the Local Group: VIII Canary Islands Winter School of Astrophysics*, ed. by A. Aparicio, A. Herrero, F. Sanchez (Cambridge University Press, Cambridge, 1998) pp. 95–147
49. P. Massey, A.B. Thompson: *AJ* **101**, 1408 (1991)
50. J.K. McCarthy, D.J. Lennon, K.A. Venn, R.P. Kudritzki, J. Puls, F. Najarro: *ApJ* **455**, L135 (1995)
51. J.K. McCarthy, R.P. Kudritzki, D.J. Lennon, K.A. Venn, J. Puls: *ApJ* **482**, 757 (1997)
52. G. Meynet, A. Maeder, G. Schaller, D. Schaerer, C. Charbonnel: *A&AS* **103**, 97 (1994)
53. G. Meynet, A. Maeder: *A&A* **361**, 101 (2000)
54. C.G. Millward, G.A.H. Walker: *ApJS* **57**, 63 (1985)

55. B. Muschielok et al.: A&A **352**, L40 (1999)
56. R.M. Petrie: Publications of the Dominion Astrophysical Observatory **12**, no. 9, 317 (1965)
57. M. Pierce, R.D. McClure, R. Racine: ApJ **393**, 523 (1992)
58. G. Pietrzynski, W. Gieren, P. Fouqué, F. Pont: AJ **123**, 789 (2002)
59. G. Piotto, M. Capaccioli, F. Bresolin: Memorie della Società Astronomica Italiana **63**, 465 (1992)
60. N. Przybilla (private communication)
61. N. Przybilla, K. Butler, S.R. Becker, R.P. Kudritzki: A&A **369**, 1009 (2001)
62. N. Przybilla, K. Butler: A&A **369**, 955 (2001)
63. J. Puls et al.: A&A **305**, 171 (1996)
64. J. Puls, T. Repolust, T. Hoffmann, A. Jokuthy, R. Venero: ‘Advances in Radiatively Driven Wind Models’. In: *A Massive Star Odyssey, from Main Sequence to Supernova, Proceedings of IAU Symposium No. 212*, ed. by K.A. van der Hucht, A. Herrero, C. Esteban (ASP, San Francisco, 2003) in press
65. J.D. Rosendhal: ApJ **186**, 909 (1973)
66. J.D. Rosendhal: ApJ **187**, 261 (1974)
67. J. Rousseau, N. Martin, L. Prevot, E. Rebeiro, A. Robin, J.P. Brunet: A&AS **31**, 243 (1978)
68. R. Rozanski, M. Rowan-Robinson: MNRAS **271**, 530 (1994)
69. A. Sandage, G. Carlson, J. Kristian, A. Saha, L. Labhardt: AJ **111**, 1872 (1996)
70. A. Sandage: ‘Brightest Stars in Galaxies as Distance Indicators’. In *Luminous Stars and Associations in Galaxies, Proceedings of IAU Symposium No. 116*, ed. by C.W.H. De Loore et al. (Reidel, Dordrecht, 1986) pp. 31–41
71. A. Sandage, G.A. Tammann: ApJ **191**, 603 (1974)
72. A.E. Santolaya-Rey, J. Puls, A. Herrero: A&A **323**, 488 (1997)
73. H. Schild, A. Maeder: A&A **127**, 238 (1983)
74. T. Shanks, N.R. Tanvir, J.V. Major, A.P. Doel, C.N. Dunlop, R.M. Myers: MNRAS **256**, 29 (1992)
75. M.E. Sharina, I.D. Karachentsev, N.A. Tikhonov: Astronomy Letters **25**, 322 (1999)
76. S.J. Smartt, P.A. Crowther, P.L. Dufton, D.J. Lennon, R.P. Kudritzki, A. Herrero, J.K. McCarthy, F. Bresolin: MNRAS **325**, 257 (2001)
77. Y.-J. Sohn, T.J. Davidge: AJ **115**, 130 (1998)
78. Y.-J. Sohn, T.J. Davidge: AJ **112**, 2559 (1996)
79. Y.-J. Sohn, T.J. Davidge: AJ **111**, 2280 (1996)
80. O. Struve: ApJ **69**, 173 (1929)
81. C. Trundle, P.L. Dufton, D.J. Lennon, S.J. Smartt, M.A. Urbaneja: A&A **395**, 519 (2002)
82. R.B. Tully, S.C. Wolff: ApJ **281**, 67 (1984)
83. R.B. Tully, J.M. Nakashima: ‘Distances Using A Supergiant Stars’. In *Galaxy Distances and Deviations from Universal Expansion*, ed. by B.F. Madore, R.B. Tully (Reidel, Dordrecht, 1986) pp. 25–28
84. M.A. Urbaneja, A. Herrero, R.P. Kudritzki, F. Bresolin, L.J. Corral, J. Puls: A&A **386**, 1019 (2002)
85. M.A. Urbaneja, A. Herrero, F. Bresolin, R.P. Kudritzki, W. Gieren, J. Puls: ApJ, submitted (2003)
86. A.M. van Genderen: A&A **208**, 135 (1989)
87. A.M. van Genderen: A&A **366**, 508 (2001)
88. K.A. Venn, J.K. McCarthy, D.J. Lennon, N. Przybilla, R.P. Kudritzki, M. Lemke: ApJ **541**, 610 (2001)
89. E. Verdugo, A. Talavera, A.I. Gomez de Castro: A&AS **137**, 351 (1999)
90. J.S. Vink, A. de Koter, H.J.G.L.M. Lamers: A&A **362**, 295 (2000)
91. J.S. Vink, A. de Koter, H.J.G.L.M. Lamers: A&A **369**, 574 (2001)



- 92. G.A.H. Walker, C.G. Millward: *ApJ* **289**, 669 (1985)
- 93. E.T.R Williams: 'A Spectrophotometric Study of Class A Stars. In: *Proceedings of the National Academy of Sciences of the United States of America* **15**, no. 11, 832 (1929)
- 94. D. Zaritsky, R.C. Kennicutt, J.P. Huchra: *ApJ* **420**, 87 (1994)
- 95. E. Zhang: *AJ* **88**, 825 (1983)
- 96. F.-J. Zickgraf, T. Szeifert, R.M. Humphreys: *A&A* **312**, 419 (1996)